Dyes and Pigments 214 (2023) 111190

Contents lists available at ScienceDirect

Dyes and Pigments

journal homepage: www.elsevier.com/locate/dyepig

Luminescent furo[2,3-*c*]isoquinolines as fluorophores - Tuning the luminophore by donor substitution

Lisa Moni [a], Franziska Merkt-Tasch [b], Bernhard Mayer [b], Sergio Mulone [a], Thomas J.J. Müller [b,**], Renata Riva [a,*]

[a] Dipartimento di Chimica e Chimica Industriale, Università di Genova, Via Dodecaneso 31, 16146, Genova, Italy
[b] Institut für Organische Chemie und Makromolekulare Chemie, Heinrich-Heine-Universität Düsseldorf, Universitätsstraße 1, D-40225, Düsseldorf, Germany

ARTICLE INFO

Keywords:
Fluorescence
Photochromism
One-pot reaction
Ugi reaction

ABSTRACT

A new library of the uncommon furo[2,3-*c*]isoquinoline scaffold has been synthesized by coupling the Ugi multicomponent reaction with a complex one-pot Pd-mediated double cyclization. The highly convergent and diversity-oriented approach has been exploited to introduce substituents with electron donor properties directly linked to the scaffold in the most representative positions 1 and/or 8. Moreover, the influence of an aromatic ring used as spacer between the scaffold and the electron donor substituent, as well as the substitution of the phenyl substituent in position 1 with a thiophene, on the photophysical properties have been investigated. Upon UV excitation part of the new molecules are intensively blue luminescent but for an amino donor substituent a significant switch to green emitters has been observed even upon eyesight. The electronic structure has been semiquantitatively rationalized by DFT and (TD)DFT calculations.

1. Introduction

Novel fluorophores are as functional π-electron systems [1,2] important constituents for organic light emitting diodes (OLED) [3] or as sensor molecules in biophysical analytics [4–6]. Therefore, a steady quest for tailor-made luminophores with tailored electronic properties, such as large Stokes shifts, blue emission and emission at short wavelength, i.e. blue luminescence [7,8], is constantly challenging organic synthesis. As already established in pharmaceutical lead discovery [9–14], diversity-oriented synthesis of functional chromophores [2,15,16] has increasingly become an enabling tool for exploring structural and functional space in luminophore chemistry. In particular, multicomponent reactions (MCRs) [17–28] initiated by transition metal catalyzed processes [29–31] open novel and concise alleys to heterocyclic structures [32–37], notably to fluorophores [38–41]. Domino reactions [42–47], such as a domino insertion-coupling sequence of alkynoyl *ortho*-iodo anilides and alkynes to give indolone-based scaffolds, have turned out to be particularly advantageous for establishing intensively luminescent spirocyclic butadiene chromophores [48,49] as well as proto- and metallochromic luminescent pyranoindoles [50–52]. Mechanistically, the synthesis of these fluorophores always commences via insertion-coupling formation of propynylidene indolones, which are in their own right solid-state emissive chromophores [53].

This sequence prompted us to probe Ugi-4CR substrates for six-ring anellations via the insertion-alkynylation sequel. Quite remarkably, a reductive post-Ugi Heck-transformation of Ugi-4CR products provided access to a substance library of blue emissive 3-hydroxyisoquinolines [54]. This inspired us to develop a Pd-catalyzed insertion-alkynylation-cycloisomerization domino reaction of the Ugi-4CR substrates to efficiently furnish blue emissive furo[2,3-*c*]isoquinolines, which can be fine tuned in their emission characteristics [55]. Herein, we expand the synthetic approach to donor-substituted furo[2,3-*c*]isoquinolines with isoquinoline specific donor-tuned emission that is scrutinized by photophysical measurements and (TD)DFT calculations.

2. Experimental part

2.1. General methods

NMR spectra were taken at room temperature in $CDCl_3$ or DMSO-d_6 at 300, 400 or 600 MHz (^{1}H) and 75, 101, or 151 MHz (^{13}C) by using as internal standards: in $CDCl_3$ tetramethylsilane (TMS) for ^{1}H NMR

* Corresponding author.
** Corresponding author.
E-mail addresses: ThomasJJ.Mueller@uni-duesseldorf.de (T.J.J. Müller), renata.riva@unige.it (R. Riva).

https://doi.org/10.1016/j.dyepig.2023.111190
Received 1 February 2023; Accepted 25 February 2023
Available online 28 February 2023
0143-7208/© 2023 The Authors. Published by Elsevier Ltd. This is an open access article under the CC BY license (http://creativecommons.org/licenses/by/4.0/).

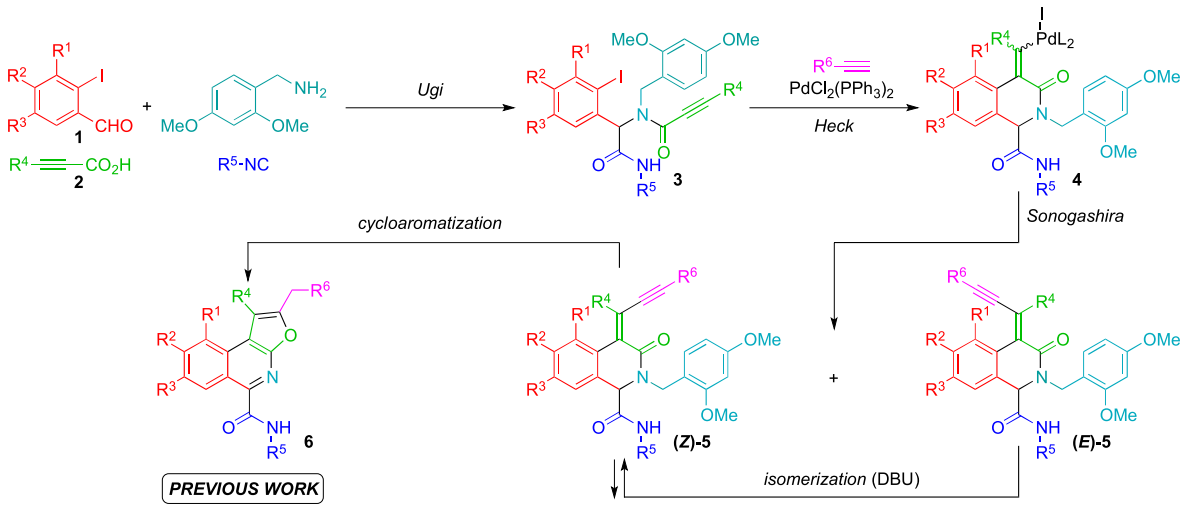

Scheme 1. Synthesis of the first generation library of furo[2,3-c]isoquinolines **6**.

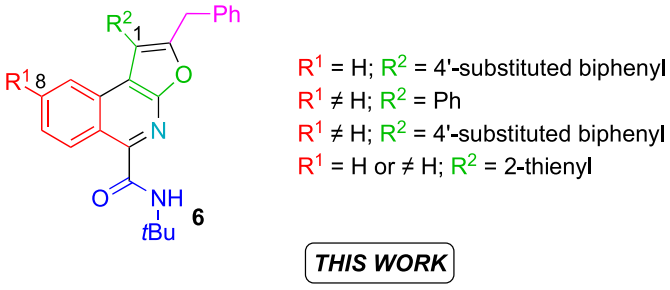

Fig. 1. Planning the new library.

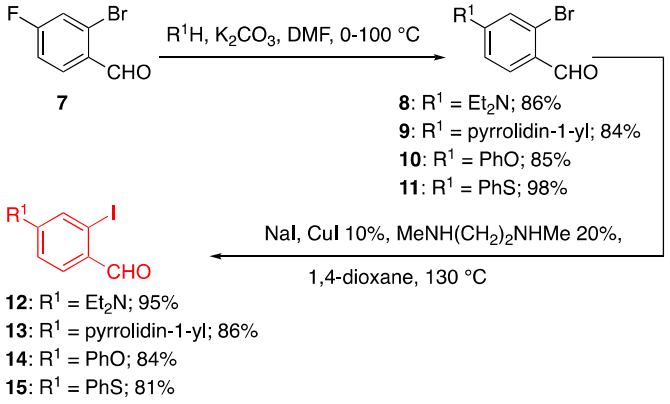

Scheme 2. Synthesis of 2-iodobenzaldehydes **12**–**15**.

spectroscopy and the central peak of $CDCl_3$ (at $\delta = 77.16$) for ^{13}C NMR spectroscopy. Chemical shifts are reported in ppm (δ scale), coupling constants are reported in Hertz. Peak assignments were also made with the aid of gCOSY and gHSQC experiments. TLC analyses were carried out on silica gel plates and viewed at UV ($\lambda = 254$ nm or 360 nm) and developed with Hanessian stain (dipping into a solution of $(NH_4)_4MoO_4{\cdot}4H_2O$ (21 g) and $Ce(SO_4)_2{\cdot}4H_2O$ (1 g) in concentrated H_2SO_4 (31 mL) and H_2O (469 mL) and warming) or with potassium permanganate reagent (solution prepared dissolving potassium permanganate in distilled water until appearance of deep purple color). R_f values were measured after an elution of 7–9 cm. Absorption spectra were recorded in CH_2Cl_2 UVASOL® at 293 K on a Perkin Elmer UV/VIS/NIR Lambda 19 Spectrometer. Emission spectra were recorded in CH_2Cl_2 UVASOL® or cyclohexane UVASOL® at 293 K on a Hitachi F7000 spectrometer. The molar extinction coefficients and quantum yields were carried out in a multipoint set up. The quantum yields are measured relative to 9,10-diphenylanthracene. All spectra are normalized to arbitrary units. HRMS analyses were performed using the ionization method ESI+ with a Bruker Daltonics maXis 4G high resolution mass spectrometer with an UHR-QTOF analyzer. Elemental analyses were measured on the Perkin Elmer Series II Analyzer 2400 at the Institute of Pharmaceutical Chemistry, Heinrich Heine University Düsseldorf. Column chromatography was done with the "flash" methodology by using 220–400 mesh silica or by means of a Biotage SP4 robot using Interchim Puriflash PF-50SIHP-JP 80 g columns. Petroleum ether (40–60 °C) is abbreviated as PE. All reactions employing dry solvents were carried out under nitrogen or argon atmosphere.

2.2. *Typical procedure for the synthesis of Ugi compounds* ***3***

N-(2-(tert-Butylamino)-1-(3-iodo-4′-methoxy-[1,1′-biphenyl]-4-yl)-2-oxoethyl)-N-(2,4-dimethoxybenzyl)-3-phenylpropiolamide **3e**: A solution of 3-iodo-4′-methoxy-[1,1′-biphenyl]-4-carbaldehyde (**22**) (135 mg, 0.40 mmol) in dry methanol/ethanol (1:1, 1.8 mL) under a nitrogen atmosphere, was treated with 2,4-dimethoxybenzylamine (64 μL, 0.42 mmol) and molecular sieves 3 Å (20 mg, activated by a night in oven at 130 °C). After 1 h, the solution was treated with phenylpropiolic acid (61 mg, 0.42 mmol) and *tert*-butyl isocyanide (47 μL, 0.42 mmol), and stirred at 40 °C. After 24 h, the mixture was filtered through a celite cake, washing with CH_2Cl_2, and the crude was purified by column chromatography (PE/EtOAc 2:1) obtaining **3e** as a pale-yellow solid (256 mg, 89%). R_f 0.30 (PE/EtOAc 2:1). Mp 124.3–125.9 °C (CH_2Cl_2). ^1H NMR (300 MHz, $CDCl_3$, 25 °C, TMS): $\delta =$ (72:28 mixture of rotamers; the prevailing is indicated as "M", while the minor is indicated as "m") 7.99 (m) (d, $J = 1.9$ Hz, 1H, H Ar), 7.85 (M) (d, $J = 1.7$ Hz, 1H, H Ar), 7.59 (M) (dd, $J = 8.2$, 1.5 Hz, 1H, H Ar), 7.52–7.26 (M + m) (m, 18 H, H Ar), 7.16 (M) (d, $J = 8.4$ Hz, 1H, H Ar), 7.01–6.92 (M + m) (m, 2H, H Ar), 6.40 (m) (dd, $J = 8.5$, 2.4 Hz, 1H, H Ar), 6.35 (M) (dd, $J = 8.4$, 2.4 Hz, 1H, H Ar), 6.29 (m) (d, $J = 2.4$ Hz, 1H, H Ar), 6.19 (M) (d, $J = 2.4$ Hz, 1H, H Ar), 6.13 (m) (s, 1H, CHNH), 5.84 (m) (broad s, 1H, NH), 5.71 (M) (s, 1H, CHNH), 5.59 (M) (broad s, 1H, NH), 4.99 and 4.80 (M) (AB syst., $J = 16.1$ Hz, 2H, CH_2DMB), 4.79 and 4.21 (m) (AB syst., $J = 15.0$ Hz, 2H, CH_2DMB), 3.85 (M + m) (s, 6H, CH_3O), 3.76 (m) (s, 3H, CH_3O), 3.72 (M) (s, 3H, CH_3O), 3.66 (m) (s, 3H, CH_3O), 3.65 (M) (s, 3H, CH_3O), 1.30 (M) (s, 9H, 3 CH_3 *t*Bu), 1.18 (m) (s, 9H, 3 CH_3 *t*Bu). ^{13}C NMR (75 MHz, $CDCl_3$) (72:28 mixture of rotamers) δ 167.9 (Cq), 167.4 (Cq), 160.6 (Cq), 160.4 (Cq), 159.73 (Cq), 159.68 (Cq), 157.85 (Cq), 157.82 (Cq), 157.2 (Cq), 156.2 (Cq), 142.6 (Cq), 142.4 (Cq), 137.5 (CH), 135.5 (CH), 135.2

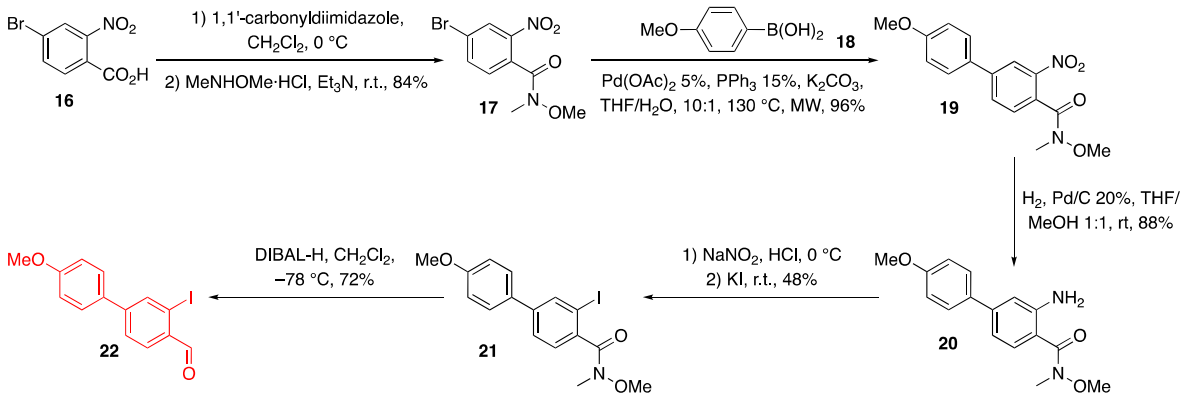

Scheme 3. Synthesis of 2-iodoarylaldehyde **22**.

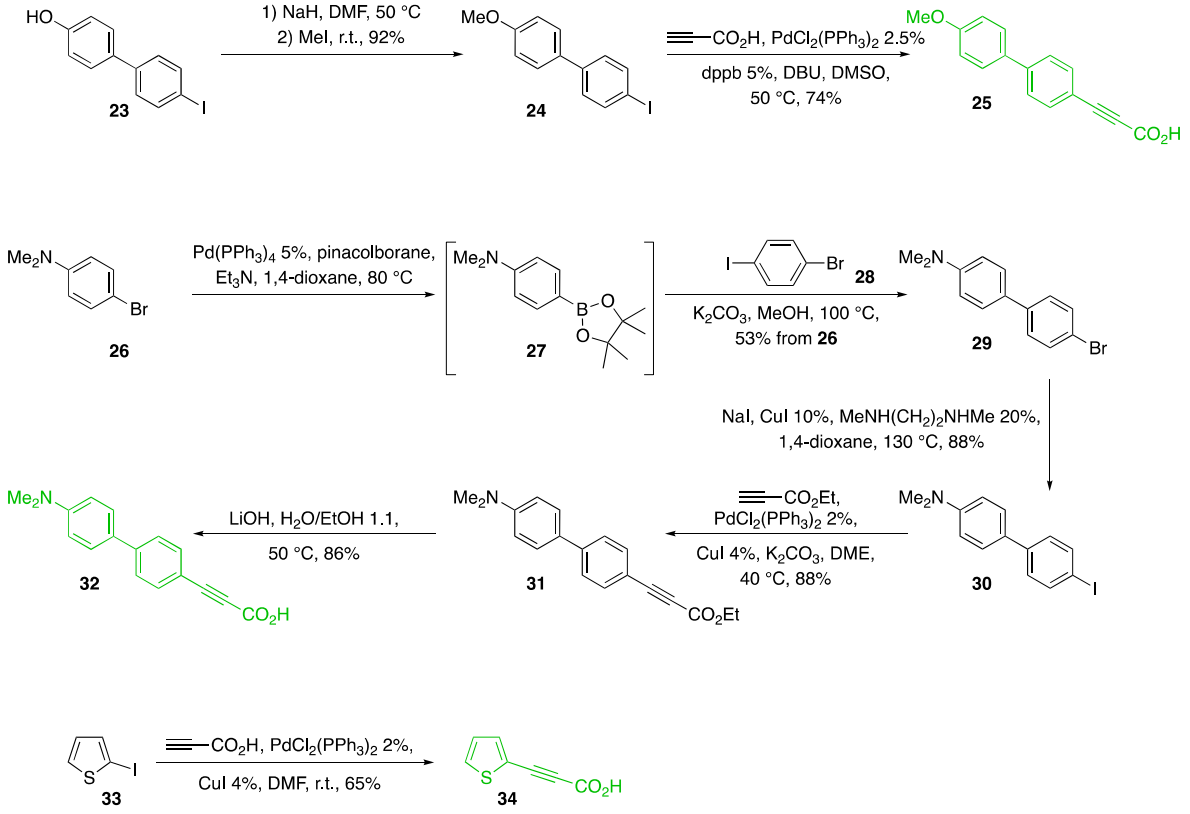

Scheme 4. Synthesis of propiolic acids **25**, **32** and **34**.

(Cq), 132.9 (CH), 132.5 (CH), 132.1 (CH), 131.3 (CH), 131.2 (CH), 130.8 (CH), 130.5 (CH), 130.4 (CH), 130.0 (CH), 128.5 (2 CH), 128.2 (2 CH), 126.1 (CH), 125.9 (CH), 120.6 (Cq), 117.9 (Cq), 117.0 (Cq), 114.4 (2 CH), 104.7 (CH), 104.1 (CH), 103.6 (Cq), 103.4 (Cq), 98.2 (CH), 97.8 (CH), 90.5 (Cq), 82.3 (Cq), 82.0 (Cq), 67.6 (CH), 55.4 (CH_3), 55.1 (2 CH_3O), 51.6 (Cq), 51.5 (Cq), 47.1 (CH_2), 28.5 (3 CH_3 *t*Bu), 28.3 (3 CH_3 *t*Bu). HRMS (ESI+): *m/z* calcd for $C_{37}H_{38}IN_2O_5$ $[M+H]^+$: 717.1820. Found: 717.1820.

2.3. Typical procedure for the synthesis of furo[2,3-c]isoquinolines 6

2-Benzyl-N-(tert-butyl)-8-(4-methoxyphenyl)-1-phenylfuro [2,3-c] isoquinoline-5-carboxamide **6e**: A solution of **3e** (125 mg, 0.17 mmol) in MeCN/Et_3N (1:1, 2 mL) under an argon atmosphere was treated with $PdCl_2(PPh_3)_2$ (7 mg, 9 μmol) and phenylacetylene (40 μL, 0.35 mmol) at 90 °C with microwaves heating for 1 h. Then, DBU (26 μL, 0.17 mmol) was added and the mixture was stirred at 110 °C (MW heating, 60 W) for 1 h. Afterwards, the reaction was diluted with CH_2Cl_2, washed with saturated aqueous NH_4Cl, dried (Na_2SO_4), and concentrated. The crude was eluted from a column of silica gel with PE/EtOAc (8:1) to give **6e** (58 mg, 61%) as a yellow solid. R_f 0.28 (PE/EtOAc 8:1). Mp 189.6–190.7 °C (CH_2Cl_2). ^{1}H NMR (300 MHz, $CDCl_3$) δ 9.73 (d, J = 9.2 Hz, 1H, H Ar), 7.95 (broad s, 2H, H Ar + NH), 7.78 (dd, J = 9.2, 1.9 Hz, 1H, H Ar), 7.60–7.51 (m, 5H, H Ar), 7.40 (d, J = 8.8 Hz, 2H, 2 H Ar), 7.34–7.19 (m, 5H, H Ar), 6.91 (d, J = 8.8 Hz, 2H, 2 H Ar), 4.16 (s, 2H, CH_2), 3.83 (s, 3H, CH_3O), 1.56 (s, 9H, 3 CH_3 *t*Bu). ^{13}C NMR (75 MHz, $CDCl_3$) δ 165.5 (C═O), 159.9 (Cq), 154.8 (Cq), 153.9 (Cq), 143.5 (Cq), 141.2 (Cq), 137.3 (Cq), 133.6 (Cq), 132.5 (Cq), 132.0 (Cq), 130.5 (2 CH), 129.7 (CH), 128.9 (2 CH), 128.73 (2 CH), 128.66 (2 CH), 128.4 (CH), 128.3 (2 CH), 126.8 (CH), 125.1 (CH), 123.8 (Cq), 119.7 (Cq), 119.0 (CH), 116.0 (Cq), 114.4 (2 CH), 55.4 (OCH_3), 51.3 (Cq), 32.9 (CH_2), 28.8 (3 CH_3 *t*Bu). HRMS (ESI+): *m/z* calcd for $C_{36}H_{33}N_2O_3$

Table 1
Synthesis of the second-generation library of compounds **6**.

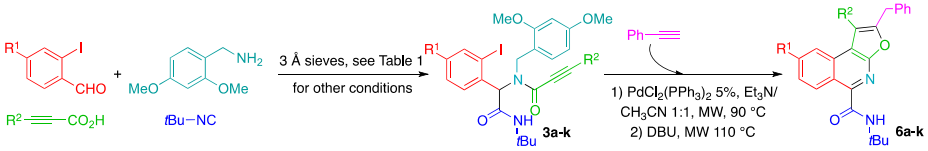

Entry	R^1	R^2	Compound[a]	Yield **3** (%)	Compound	Yield **6** (%)
1	H[b]	4′-MeO–C_6H_4–C_6H_4[c]	**3a**	70	**6a**	65
2	H[b]	4′-Me_2N–C_6H_4–C_6H_4[c]	**3b**	79	**6b**	50
3	Et_2N[d]	Ph[e]	**3c**	84	**6c**	43
4	pyrrolidin-1-yl[d]	Ph[e]	**3d**	87	**6d**	38
5	4-MeO-C_6H_4[d]	Ph[e]	**3e**	90	**6e**	68
6	PhO[d]	Ph[e]	**3f**	92	**6f**	58
7	PhS[d]	Ph[e]	**3g**	82	**6g**	29
8	4-MeO-C_6H_4[d]	4′-MeO–C_6H_4–C_6H_4[c]	**3h**	67	**6h**	77
9	Et_2N[d]	4′-MeO–C_6H_4–C_6H_4[c]	**3i**	69	**6i**	40
10	H[b]	2-thienyl[c]	**3j**	63	**6j**	58
11	Et_2N[d]	2-thienyl[c]	**3k**	60	**6k**	48

Notes: [a] Ugi reactions conditions: **3a** (EtOH/2,2,2-trifluoroethanol 1:1, 40 °C), **3b**, **3c**, **3i** and **3k** (MeOH, 45 °C), **3d**, **3h** and **3j** (MeOH, 40 °C), **3e** (MeOH/EtOH 1:1, 40 °C), **3f** (MeOH, r.t.), **3g** (MeOH/EtOH 1:1, 45 °C); [b] 2-iodobenzaldehyde prepared according to a previously described procedure [54]; [c] acids: **25** (R^2 = 4′-MeO–C_6H_4–C_6H_4), **32** (R^2 = 4′-Me_2N–C_6H_4–C_6H_4), **34** (R^2 = 2-thienyl); [d] aldehydes: **12** (R^1 = Et_2N), **13** (R^1 = pyrrolidin-1-yl), **14** (R^1 = PhO), **15** (R^1 = PhS), **22** (R^1 4-MeO-C_6H_4); [e] commercially available acid.

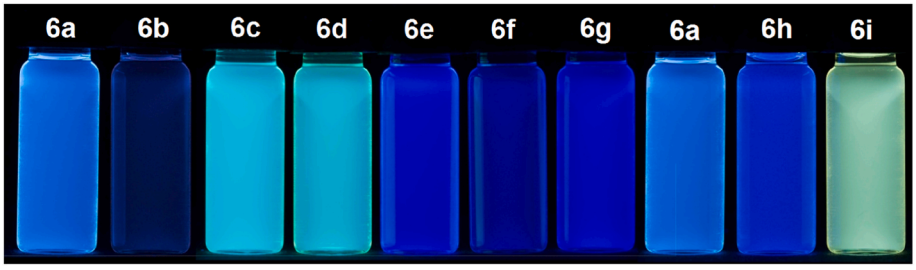

Fig. 2. Apparent fluorescence of dichloromethane solutions of selected furo[2,3-*c*]isoquinolines **6** under the handheld UV lamp (recorded at $T = 293$ K, $c(6) \sim 10^{-5}$ M, $\lambda_{exc} \approx 365$ nm).

$[M+H]^+$: 541.2486. Found: 541.2481.

3. Results and discussion

3.1. Synthesis

We recently developed an efficient synthesis of furo[2,3-*c*]isoquinoline scaffold **6** [55]. This protocol requires an initial Ugi MCR where 2,4-dimethoxybenzylamine is used as ammonia surrogate to afford **3** (Scheme 1). The addition of a terminal alkyne and a Pd(II) species to **3** allows the cascade sequence to start: after an intramolecular Heck-type insertion reaction the intermediate vinyl palladium species **4** is trapped by the alkyne in a Sonogashira reaction to afford a mixture of **(*Z*)-5** and **(*E*)-5**; eventually the cycloaromatization of the former affords **6**, with simultaneous loss of the 2,4-dimethoxybenzyl fragment. The ineffective **(*E*)-5** diastereomer, resulting from a poorly stereoselective Heck reaction, could be easily isomerized *in situ* to **(*Z*)-5** under basic conditions (addition of 1,8-diazabicyclo[5.4.0]undec-7-ene, i.e. DBU) and thus recycled.

Scaffold **6** demonstrated to be highly blue emissive upon excitation in the ultraviolet and, to understand the influence of the substituents on the photophysical properties, we varied the structures of three out of four components of the Ugi reaction because the structure of the amine is necessarily fixed. In particular we investigated the factors affecting the photoluminescence, due to the presence of electron withdrawing (EWG) and/or electron releasing (ERG) groups placed on the aldehyde **1** and on the aryl propiolic acid **2**. On the contrary R^5 (isocyanide) and R^6 (terminal alkyne for the Sonogashira reaction) demonstrated to have a negligible influence because they are not involved in the conjugation with the heteroaromatic scaffold.

The photophysical characterization by absorption and emission spectroscopy revealed that the emission wavelength, Stokes shift, as well as fluorescence quantum yield depend mostly on the presence of donor substituents on the isoquinoline moiety, in particular if placed on C_8 and, albeit to a lesser extent, by the substituent in position 4 of the aryl bound to C_1.

In this work we focussed our attention on the synthesis of a second-generation library of compounds **6**, varying the substitution pattern on the furoisoquinoline scaffold (Fig. 1) with two main purposes: a) better understand the influence of the substituents on C_8 and C_1 on the photophysical properties and possibly shift to green or even red emitters; b) study the influence of the substitution of aryl on C_1 with a small heteroaryl, such as thiophene. Actually, previous DFT calculations demonstrated a torsional angle of $\theta_{calc} = 72°$ between the furoisoquinoline moiety and the 1-aryl substituent which can in part diminish the electronic communication between both aromatic systems [55]; switching to thiophene is expected to diminish this angle.

Among the possible structures we have identified four different combinations of the substituents as summarized in Fig. 1. This required in most cases a custom-made synthesis of the appropriate 2-iodobenzaldehyde **1** (R^1) and propiolic acid **2** (R^2).

For the synthesis of aldehydes **8**–**11** with an ERG in the *para* position with respect to the carbonyl we followed the same strategy, that is an aromatic nucleophilic substitution on 2-bromo-4-fluorobenzaldehyde **7** with the appropriate nucleophile to install a diethylamino (**8**) or a pyrrolidin-1-yl group (**9**) [56], as well as a phenoxy (**10**) or a

Table 2
Photophysical properties of the furo[2,3-*c*]isoquinolines **6** ($T = 293$ K).

Entry	Compound	$\lambda_{max,abs}$ [nm] (ε) [L mol^{-1} cm^{-1}])[a]	$\lambda_{max,em}$ [nm] (Φ_F [a.u.])[b]	Stokes shift ($\Delta\tilde{\nu}$[cm^{-1}])[c]
1	**6a**	259.0 (26100) 354.0 (16700)	448.0 (0.60)[d]	5900
2	**6b**	318.0 (24600) 352.0 (20400)	410.0 (0.02)[d]	4000
3	**6c**	255.5 (25000sh) 282.0 (26000) 345.0 (7930) 399.0 (9830)	477.5 (0.24)[e]	4100
4	**6d**	255.5 (25000sh) 283.0 (26700) 346.0 (8300) 399.5 (10000)	477.0 (0.24)[e]	4100
5	**6e**	282.0 (35100) 359.0 (18300)	425.0 (0.26)[d]	4300
6	**6f**	272.0 (22800) 353.0 (12700)	426.5 (0.03)[d]	4900
7	**6g**	259.0 (37300) 348.0 (13300)	411.0 (0.38)[d]	4400
8	**6h**	280.5 (49600) 359.0 (17700)	430.0 (0.22)[d]	4600
9	**6i**	255.0 (29800) 279.0 (39200) 342.0 (10000sh) 399.0 (8200)	477.0 (0.27)[e]	4100
10	**6j**	353.0 (19700)	447.0 (<0.01)[e]	6000
11	**6k**	253.0 (21300) 284.0 (18900) 331.0 (sh) (5700) 345.5 (6300) 401.0 (8200)	496.0 (0.47)[e]	4800

Notes: [a] Recorded in CH_2Cl_2, $c = 10^{-5}$ M at $T = 293$ K; [b] quantum yields were determined employing literature procedures [64]; [c] $\Delta\tilde{\nu} = 1/\lambda_{max,abs} - 1/\lambda_{max,em}$; [d] 9,10-diphenylanthracene as a standard in cyclohexane ($\Phi_F = 1.00$) [65], recorded in CH_2Cl_2 at r.t. with $\lambda_{exc} = 350$ nm, $c = 10^{-7}$ m; [e] coumarin 30 as a standard in acetonitrile ($\Phi_F = 0.67$) [66], recorded in CH_2Cl_2 at r.t. with $\lambda_{exc} = 380$ nm, $c = 10^{-7}$ M.

thiophenoxy (**11**) group [57] (Scheme 2). Since the Heck-Sonogashira-cycloaromatization protocol does not work on aryl bromides a halogen exchange to iodide was necessary, which was realized using the aromatic copper-catalyzed Finkelstein reaction to afford **12**–**15** [58].

To synthesize the biphenyl iodoaldehyde **22** we had to follow an *ad hoc* planned strategy (Scheme 3). We transformed commercially available 4-bromo-2-nitrobenzoic acid **16** into the corresponding Weinreb amide **17**, a synthetic equivalent of the aldehyde group. The biphenyl moiety (**19**) was assembled through a Suzuki coupling with boronic acid **18**. After hydrogenation of the nitro group, amine **20** was transformed into iodide **21**, through a Sandmeyer-like reaction [59], and eventually the selective reduction of the Weinreb amide with 1 equivalent of DIBAL-H afforded aldehyde **22** without halide reduction.

As for the synthesis of propargylic acids **25** and **32** two original procedures were developed (Scheme 4). Compound **25** was prepared by methylation of commercially available **23**, and **24** was submitted to a Pd-mediated coupling with propiolic acid in the presence of 1,4-bis (diphenylphosphano)butane (dppb) as phosphane [60].

For the preparation of **32**, we submitted **26** to the one-pot Masuda borylation [61] – Suzuki coupling recently developed by us [62], where the intermediate boronate **27** reacts selectively with the more reactive iodine of **28**. Biphenyl **29** is then submitted to the aromatic Finkelstein reaction for the bromine/iodine exchange (**30**). This time the carbethoxyethynyl moiety was directly installed through an efficient Sonogashira coupling requiring the slow addition of ethyl propiolate over 20 h to give **31**, which was hydrolyzed to **32**.

For the synthesis of **34**, we slightly modified a known procedure, and coupled 2-iodothiophene **33** with propargylic acid under Sonogashira conditions [63].

With all the needed substrates we turned to the synthesis of **6** coupling the Ugi reaction with the Pd-mediated one-pot sequence, as summarized in Table 1. We preferred to employ the two-step procedure in which the Ugi product **3** has been isolated. The MCR reactions were performed under slightly different conditions (solvent and temperature) because of the different solubility in MeOH of the reagents and afforded **3** in good to excellent yield. About the Heck-Sonogashira-cycloaromatization sequence we followed the already reported protocol [55]. The yields of these complex transformations are quite variable ranging from moderate to excellent (entries 1, 5, 6, 8, 10). On the other hand, the presence of a nitrogen or a sulfur on the ERG seems to negatively affect the overall yield (entries 2–4, 7, 9, 11).

3.2. Photophysical studies

Dichloromethane solutions of selected furo[2,3-*c*]isoquinolines **6** reveal a remarkable blue and yellow-greenish fluorescence under illumination with a handheld UV lamp, visible to the naked eye (Fig. 2). Both color and intensity are strongly affected by the substitution pattern. Therefore, the photophysical properties were studied by UV/Vis and fluorescence spectroscopy for determining absorption and emission maxima, molar extinction coefficients, Stokes shifts and relative fluorescence quantum yields [64] with 9,10-diphenylanthracene [65] and coumarin 30 [66] as reference standards (Table 2).

The longest wavelength absorption maxima of the furo[2,3-*c*]isoquinolines **6** appear between 348 and 401 nm and several additional absorption bands are found at higher energies, as seen e.g. for dyes **6c**, **6d**, and **6i** (Table 2, entries 3, 4, and 10). In comparison to the previously reported furo[2,3-*c*]isoquinolines [54,55] most 8-donor substituted furo[2,3-*c*]isoquinolines **6a-i** exhibit emission maxima between 410 and 496 nm, with large Stokes shifts $\Delta\tilde{\nu}$ between 4000 and 6000 cm^{-1} and fluorescence quantum yields Φ_F ranging from 0.02 to 0.60 (Table 2).

The effect of the substitution pattern of donor substituted furo[2,3-*c*] isoquinolines can be discussed in three series with variable positioning of the donor substituents (Fig. 3).

In series 1 (Fig. 3, orange box, dyes **6a** and **6b**) the donor is remotely placed as a *p*-biphenyl substituent in position 1 of the furo[2,3-*c*]isoquinoline core. With longest wavelength absorption maxima of 354 (**6a**) and 352 nm (**6b**) the donor effect on the absorption behavior is minute, indicating almost a neglectable electronic influence (Table 2, entries 1 and 2). However, the substituent effect on the excited state as reflected by the emission maxima is quite substantial. The emission maximum of the methoxy derivative **6a** (448 nm) is bathochromically shifted by 2070 cm^{-1} in comparison to the dimethylamino derivative **6b** (410 nm), accompanied by a significantly higher fluorescence quantum yield of 0.60 (**6a**) in comparison to 0.02 (**6b**).

In series 2 (Fig. 3, green box), represented by dyes **6c-6g** the donor is directly ligated to position 8 of the furo[2,3-*c*]isoquinoline core. For series 2, the effect of the donor strength on the longest wavelength absorption band and the emission maxima becomes apparent (Table 2, entries 3–7, Fig. 4). The nitrogen donors diethylamino (**6c**) and pyrrolidin-1-yl (**6d**) are strongest and cause a considerable redshift of the absorption (399 and 399.5 nm) and emission bands (477.5 and 477 nm). The absorption and emission bands of oxygen (**6e**, **6f**) and sulfur (**6g**) donors are blue-shifted and appear between 348 and 359 nm (absorption) and 411 and 426.5 nm (emission). With exception of the phenoxy derivative **6f**, the fluorescence quantum yields in this series amount to 0.24 (**6e**) and 0.38 (**6g**). Yet, the weakest donor, i.e. phenylthio substituent (compound **6g**) gives rise to the highest quantum yield. The 1-(2′-thienyl) substituent dyes **6j** and **6k** are peculiar with respect to their emission characteristics. While dye **6j** bearing no donor substituent at position 8 almost shows no emission, its 8-diethylamino substituted congener **6k** displays the most red-shifted emission maximum of all furo[2,3-*c*]isoquinolines **6** and significant increase in fluorescence quantum yield up to 0.47 accounts for a peculiar

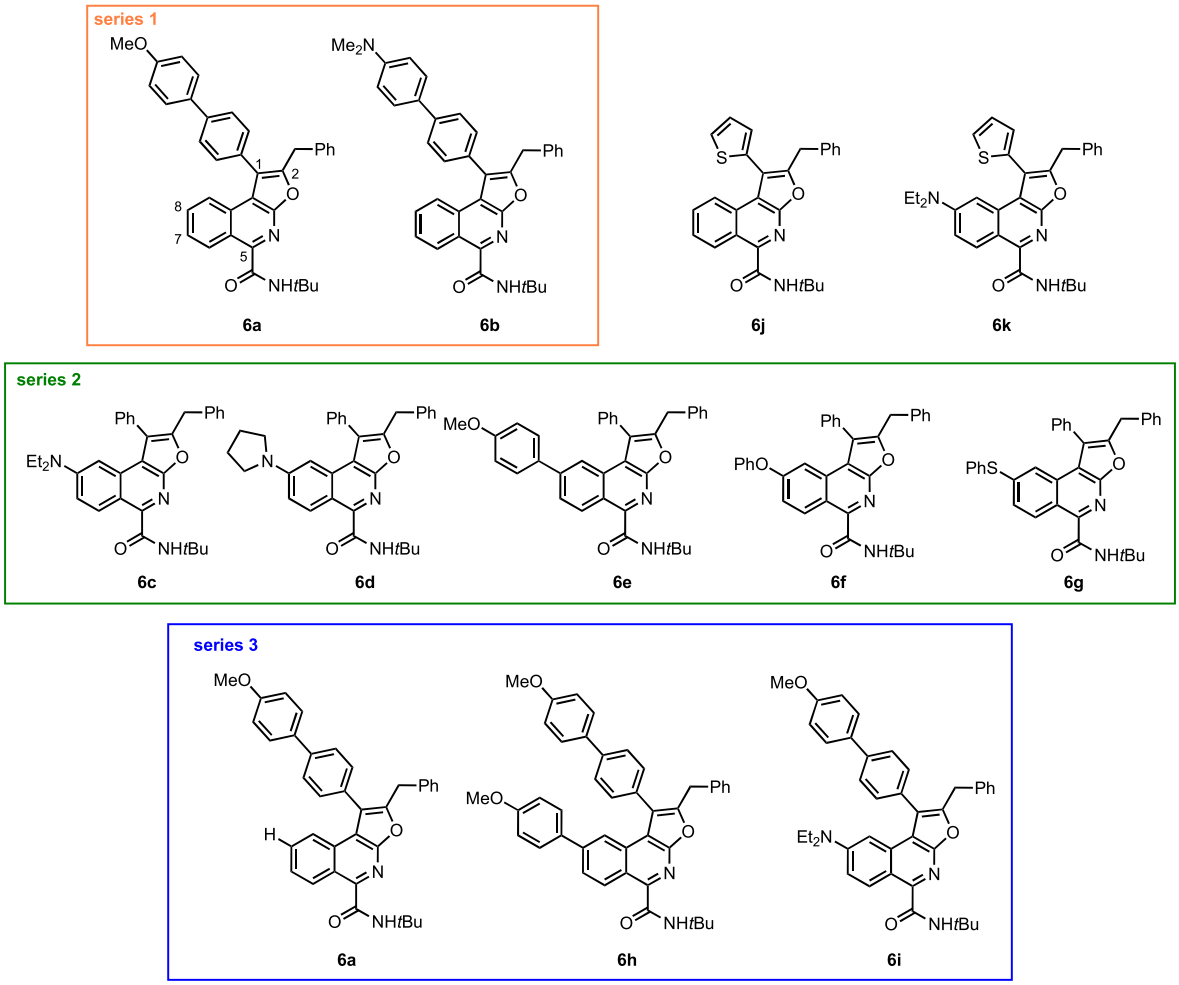

Fig. 3. Series 1, 2, and 3 of selected 1-substituted furo[2,3-*c*]isoquinolines **6**.

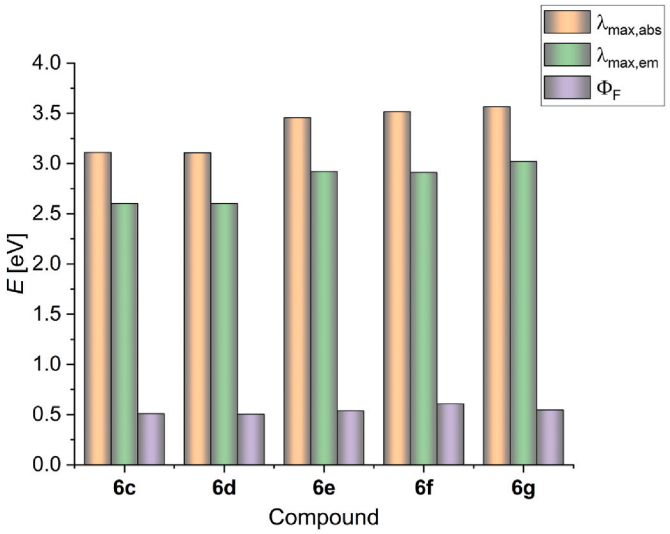

Fig. 4. Absorption maxima (orange), emission maxima (green), and Stokes shifts (purple) (energies in eV) of 8-donor-substituted furo[2,3-*c*]isoquinolines **6c-g** (Series 2).

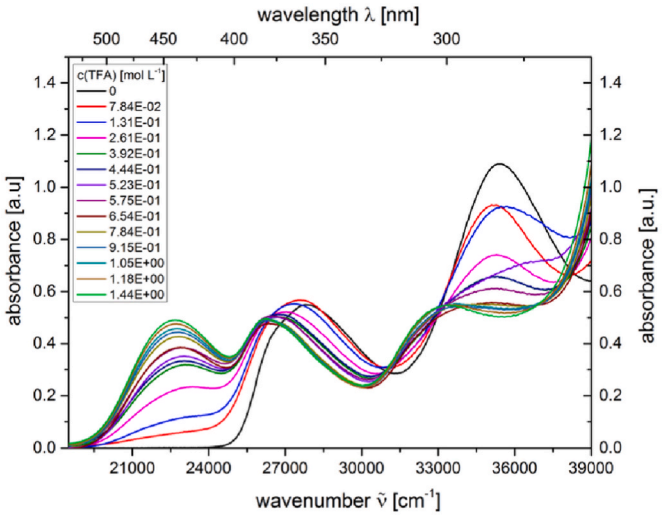

Fig. 5. UV/Vis titration of compound **6e** with TFA (recorded in CH_2Cl_2 at T = 293 K).

substituent cooperativity. The Stokes shifts in this consanguineous series amount between 4100 and 5900 cm^{-1} (0.50–0.60 eV) (Fig. 4).

In series 3 (Fig. 3, blue box), the electronic spectra of three dyes (**6a**, **6h**, and **6i**) with *p*-methoxy biphenyl substituents in position 1 and hydrogen, *p*-anisyl, and diethylamino substituents in position 8 are compared (Table 2, entries 1, 8, and 9), and this comparison reveals some interesting aspects. The placement of an additional donor causes a

Table 3
Selected experimental and first six TD-DFT calculated (B3LYP/6-31+G(d,p)) absorption maxima of **6c** and **6d** (recorded in dichloromethane, $T = 293$ K, $c(6) = 10^{-7}$ M, and calculated with polarizable continuum model (PCM) for dichloromethane as a solvent using the cLR model).

compound	$\lambda_{max,abs}$ [nm] (ε [L mol^{-1} cm^{-1}])	$\lambda_{max,calcd}$ [nm]	oscillator strength	most dominant contributions
6c	399 (9800)	419.4	0.2883	HOMO→LUMO (98%)
	345 (7900)	329.4	0.1651	HOMO-1→LUMO (72%) HOMO→LUMO+1 (7%)
		318.3	0.0015	HOMO-4→LUMO (41%) HOMO-2→LUMO (31%)
		310.4	0.0831	HOMO→LUMO+1 (81%) HOMO-1→LUMO (7%)
	282 (26000)	297.8	0.0059	HOMO→LUMO+2 (56%) HOMO→LUMO+3 (41%)
		295.1	0.1355	HOMO-2→LUMO (35%) HOMO→LUMO+2 (17%)
6d	399.5 (10000)	417.8	0.2984	HOMO→LUMO (98%)
	346.0 (8300)	328.4	0.1217	HOMO-1→LUMO (63%) HOMO→LUMO+1 (18%)
		316.5	0.091	HOMO→LUMO+1 (47%) HOMO-4→LUMO (23%)
		312.1	0.0526	HOMO-5→LUMO (39%) HOMO→LUMO+1 (30%)
	283.0 (26700)	299.8	0.0138	HOMO→LUMO+2 (78%) HOMO→LUMO+3 (20%)
		295.0	0.0947	HOMO-2→LUMO (41%) HOMO-4→LUMO (20%)

Table 4
Experimental and first TD-DFT calculated (B3LYP/6-31+G(d,p)) emission maxima of **6c** and **6d** (recorded in dichloromethane, $T = 293$ K, $c(\mathbf{6}) = 10^{-7}$ M, and calculated with polarizable continuum model (PCM) for dichloromethane as a solvent).

compound	$\lambda_{max,em}$ [nm] (Φ_F)	$\lambda_{max,calcd}$ [nm]	oscillator strength	most dominant contributions
6c	477.5 (0.24)	510.9	0.3330	HOMO→LUMO (99%)
6d	477.0 (0.24)	517.8	0.3319	HOMO→LUMO (99%)

redshift of the longest wavelength absorption bands depending on the donor strength of the substituent at position 8. While the *p*-anisyl dye **6h** only slightly red-shifts the absorption band with respect to the parent compound **6a**, this effect is quite pronounced for the stronger donor diethylamino (**6i**). The direct comparison of the absorption spectra of compounds **6c** and **6i** underlines that the absorption characteristics of chromophore **6i** is essentially the same as for compound **6c** (Table 2, entries 3 and 9). Therefore, the Franck-Condon transition from the electronic ground state is purely governed by the furo[2,3-*c*]isoquinoline chromophore without a significant contribution of the biphenyl substituent. However, the situation changes for the excited state as reflected by the emission maxima. While the parent system **6a** emits at 448 nm, where the only conjugated substituent is the *p*-methoxy biphenyl moiety in position 1, the maximum of the *p*-anisyl substituted dye **6h** is blue-shifted to 430 nm and appears at a similar energy as the related *p*-anisyl derivative **6e** (425 nm) (Table 2, entries 1 and 5). This obviously emphasizes that the emission behavior of 1,8-bisdonor-substituted furo[2,3-*c*]isoquinolines is exclusively governed by the donor substituent in position 8. This is additionally supported by the emission behavior of diethylamino derivative **6i**, where emission band appears at 477 nm, i.e. the identical energy as for the related dye **6c** (Table 2, entries 3 and 9). This assumption is further supported by comparison of the fluorescence quantum yields of series 2 and 3. The bisdonor dyes **6h** and **6i** display very similar quantum yields as their related congeners **6c** and **6e**, i.e. with values of 0.27 and 0.22 (Table 2, entries 3, 5, 8, and 9). The parent compound **6a** displays more than double in its fluorescence efficiency (Table 2, entry 1). Therefore, it can be concluded that the substituent at position 8 governs both the absorption and emission behavior, regardless how extended the π-conjugation at position 1 might be. This effect appears to be correlated to a significant torsion of the substituent at position 1 [55]. And, as shown from the absorption and emission characteristics of the 1-(2′-thienyl) substituent, in dyes **6j** and **6k** (Table 2, entries 10 and 11) the diminished torsion of the 1-substituent enhances the overlap and causes the most red-shifted absorption and emission for bisdonor-substituted dye **6k**. In turn, the torsional effect of the aryl substitution at position 1, which does not affect the luminescence efficacy can therefore be exploited as the best site for ligating furo[2,3-*c*]isoquinoline fluorophores to bioorganic ligands.

3.2.1. *Absorption protochromicity of dye **6e***

Furo[2,3-*c*]isoquinoline **6e** absorbs in the near UV and the solution is colorless at daylight; however, upon addition of a strong acid, the color bathochromically shifts to yellow. The furo[2,3-*c*]isoquinoline **6e** bears two basic sites, the isoquinoline nitrogen atom and the amide oxygen atom. Therefore, the absorption protochromicity of compound **6e** was photometrically studied by acid titration. Upon titration of dye **6e** with trifluoroacetic (TFA) a redshifted maximum at 442 nm develops while the maximum at 282 nm slowly decreases (Fig. 5). A large excess of TFA is required for complete protonation of **6e**. As a consequence, the pK_a of **6e-H**$^+$ amounts to −0.24 based on the assumption of complete dissociation of the strong acid TFA in dichloromethane. This remarkably low pK_a is typical for 1-acceptor substituted isoquinolines, as reported for 1-methylsulfinyl isoquinoline with a pK_a of 0.90 [67]. The pronounced redshift of the longest wavelength absorption band is indicative of protonation of the isoquinoline nitrogen atom, causing an increase of the acceptor strength in the donor-acceptor chromophore. However, also the presence of the amide oxygen atom chelating the proton and thereby increasing in the overall electron withdrawal cannot be completely ruled out for rationalizing this remarkably low pK_a [55]. Indeed, the acidity of protonated *N*-methylacetamide (pK_a = −0.7) [68] falls into a similar regime.

3.3. *Electronic structure of furo[2,3-c]isoquinolines **6c** and **6d***

The two 8-amino-substituted furo[2,3-*c*]isoquinolines **6c** and **6d** display most red-shifted absorptions and emissions. For elucidating the electronic structure of the electronic absorption spectra and the nature of the longest wavelength absorption bands DFT and TD-DFT calculations have been carried out using the program package of Gaussian16 [69]. with the B3LYP functional [70–74] and the Pople-6-31+G(d,p) basis set [75]. The polarizable continuum model (PCM) for dichloromethane as a solvent [76] is chosen to allow a comparison between calculated and experimentally determined optical transitions. First, the geometries of the electronic ground-state structures of the dyes **6c** and

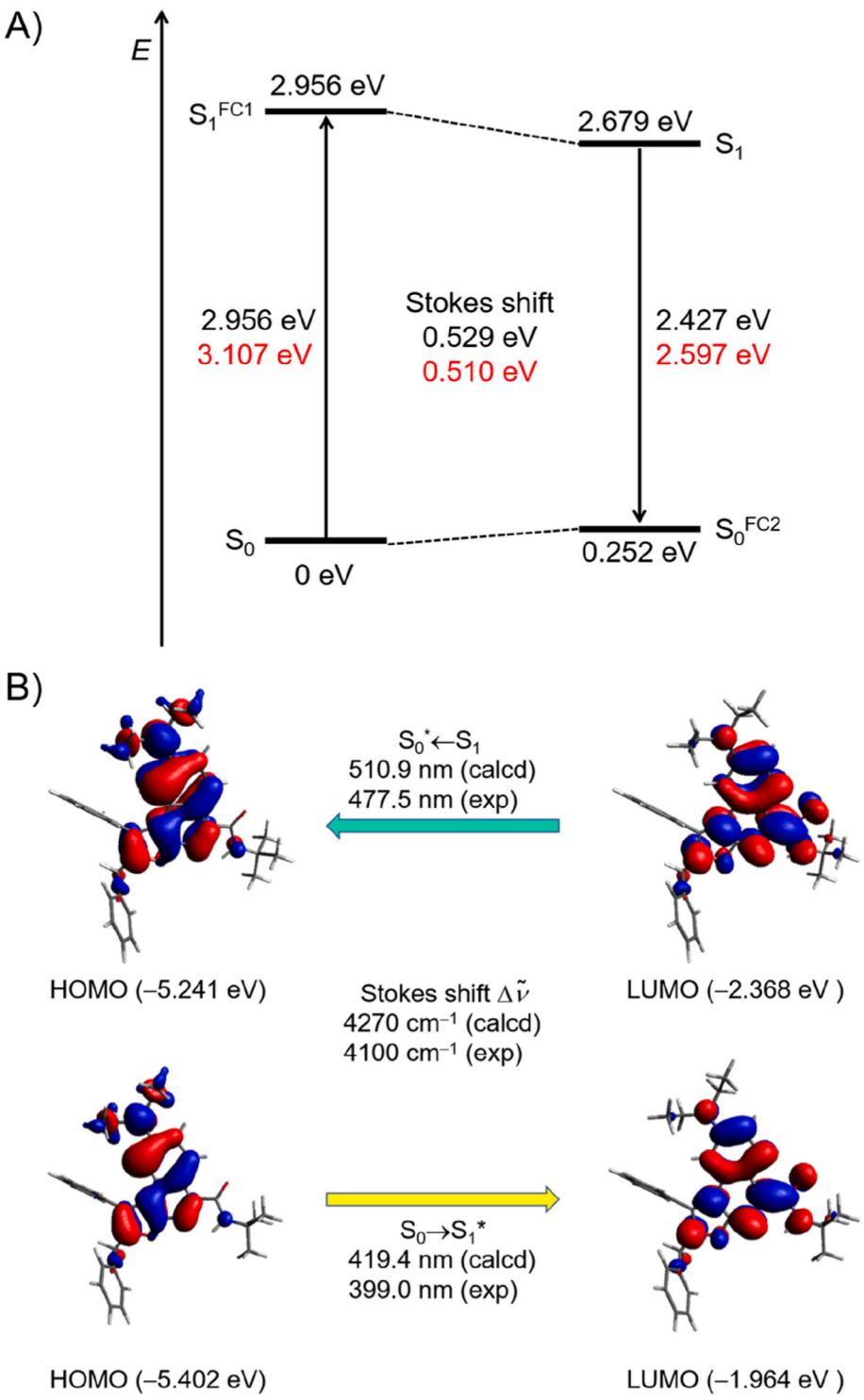

Fig. 6. Calculated excitation-relaxation-emission-relaxation cycle (A) and most relevant frontier molecular orbitals for the Franck-Condon absorption ($S_0 \rightarrow S_1^*$) and emission ($S_0^* \leftarrow S_1$) of furo[2,3-*c*]isoquinoline **6c** at the B3LYP/6-31+G(d,p) level of theory (including the PCM for dichloromethane as a solvent dielectric).

6d are optimized and all minimum structures are unambiguously confirmed by analytical frequency analyses. For determining and rationalizing the absorption characteristics, TD-DFT calculations on the S_0 ground state and the vibrationally relaxed S_1 ground state geometries are performed, again using PCM for dichloromethane as solvent and the corrected linear response (cLR) model [77] (Tables 3 and 4).

The computations reproduce the experimental obtained absorption and emission bands reasonably well. In addition, the computations allow for modelling the relaxation-excitation-relaxation-emission cycle and as shown for experimental and calculated Stokes shifts the applied TD-DFT model rationalizes the observed characteristics quite nicely (Fig. 6A and SX). Most characteristically, the longest wavelength absorption and emission bands of the furo[2,3-*c*]isoquinolines **6c** and **6d** originate from HOMO-LUMO transitions (Fig. 6B and SX). As previously shown for the second generation of furo[2,3-*c*]isoquinolines [55] and also in the experimental data of the novel series of 1,8-disubstituted congeners **6** the communication between the 1-aryl substituent and the furo[2,3-*c*]isoquinoline core in the electronic ground state is

negligible due to biaryl torsion. A closer inspection of the coefficient densities in the Kohn-Sham frontier molecular orbitals (FMO) of dyes **6c** and **6d** reveals that the benzyl substituent expectedly exerts no electronic effect on the furo[2,3-*c*]isoquinoline chromophore (Fig. 6B and SX). In addition, the absent effect influence of the 1-aryl substituent on the LUMOs is seen by the absence of coefficient density on the phenyl substituent and the node at position 1, excluding an electronic interaction of the phenyl substituent. Hence, the absorption scenario of the longest wavelength absorption bands is exclusively localized in the furo [2,3-*c*]isoquinoline core. As the amino donors at position 8 experience coefficient density in both FMOs, i.e. HOMO and LUMO, the almost identical absorption and emission bands can be plausibly rationalized. In essence for the dyes **6** it can be concluded that red-shifts of absorption and emission bands are controlled by donor substitution in position 8 with concomitant maintenance of fluorescence efficiency as shown by substantial fluorescence quantum yields.

4. Conclusions

We have described here the synthesis of a second generation library of furo[2,3-*c*]isoquinolines **6** and we have investigated thoroughly their photophysical properties. The photophysical and computational studies have revealed that the donor substituent at position 8 in the furo[2,3-*c*] isoquinoline scaffold exerts the most dominant influence on the absorption and emission behavior and also on the fluorescence efficiency and the emission tunability. Interestingly, although conjugated at position 1 the expanded biaryl substituent has almost no influence on the photophysics. In turn, this offers the option for choosing ligation to analytes, surfaces or molecules via this substituent position. The benzyl substituent on the furo moiety is neither conjugated nor affects the electronic properties of the luminophores. Therefore, new generations of furo[2,3-*c*]isoquinoline luminophores will have to take advantage of placing suitable convertible alkyne coupling partners for expanding the π-conjugation of the chromophore. Studies addressing the synthetic routes and photophysical characteristics are currently underway.

Author contribution statement

Lisa Moni: Methodology, Supervision, Writing – review & editing. Franziska Merkt: Data curation, Validation. Bernhard Mayer: DFT and TD-DFT calculations and Validation. Sergio Mulone: Investigation, Data Curation. Thomas J. J. Müller: Conceptualization, Writing – original draft, Visualization, Funding Acquisition. Renata Riva: Conceptualization, Writing – original draft, Supervision, Visualization, Funding Acquisition.

Declaration of competing interest

The authors declare that they have no known competing financial interests or personal relationships that could have appeared to influence the work reported in this paper.

Data availability

No data was used for the research described in the article.

Acknowledgements

we gratefully acknowledge Daniele Di Stefano for experimental support, the University of Genova, the Fonds der Chemischen Industrie, and the Deutsche Forschungsgemeinschaft (Mu 1088/9-1) for financial support, and the International Exchange Erasmus Student Network for a grant to S. M.

Appendix A. Supplementary data

Supplementary data to this article can be found online at https://doi.org/10.1016/j.dyepig.2023.111190.

References

[1] Levi L, Müller TJJ. Multicomponent syntheses of functional chromophores. Chem Soc Rev 2016;45(10):2825–46.
[2] Müller TJJ, Bunz UHF, editors. Functional organic materials. Syntheses, strategies, and applications. Weinheim, Germany: Wiley-VCH Verlag GmbH & Co. KGaaA; 2007.
[3] Müllen K, Scherf U, editors. Organic light emitting devices. Weinheim, Germany: Wiley-VCH Verlag GmbH & Co. KGaA; 2006.
[4] Kim E, Park SB. Chemistry as a prism: a review of light-emitting materials having tunable emission wavelengths. Chem Asian J 2009;4(11):1646–58.
[5] Cairo CW, Key JA, Sadek CM. Fluorescent small-molecule probes of biochemistry at the plasma membrane. Curr Opin Chem Biol 2010;14(1):57–63.
[6] Wagenknecht H-A. Fluorescent DNA base modifications and substitutes: multiple fluorophore labeling and the DETEQ concept. Ann N Y Acad Sci 2008;1130(1): 122–30.
[7] Yang X, Xu X, Zhou G. Recent advances of the emitters for high performance deep-blue organic light-emitting diodes. J Mater Chem C 2015;3(5):913–44.
[8] Zhu M, Yang C. Blue fluorescent emitters: design tactics and applications in organic light-emitting diodes. Chem Soc Rev 2013;42(12):4963–76.
[9] Burke MD, Schreiber SL. A planning strategy for diversity-oriented synthesis. Angew Chem Int Ed 2004;43(1):46–58.
[10] Burke MD, Berger EM, Schreiber SL. Generating diverse skeletons of small molecules combinatorially. Science 2003;302(5645):613–8.
[11] Spring DR. Diversity-oriented synthesis; a challenge for synthetic chemists. Org Biomol Chem 2003;1(22):3867–70.
[12] Arya P, Chou DTH, Baek M-G. Diversity-based organic synthesis in the era of genomics and proteomics. Angew Chem Int Ed 2001;40(2):339–46.
[13] Cox B, Denyer JC, Binnie A, Donnelly MC, Evans B, Green DV, Lewis JA, Mander TH, Merritt AT, Valler MJ, SP W. Application of high-throughput screening techniques to drug discovery. Prog Med Chem 2000;37:83–133.
[14] Schreiber SL. Target-oriented and diversity-oriented organic synthesis in drug discovery. Science 2000;287(5460):1964–9.
[15] Müller TJJ, D'Souza DM. Diversity-oriented syntheses of functional π-systems by multicomponent and domino reactions. Pure Appl Chem 2008;80(3):609–20.
[16] Briehn CA, Bäuerle P. From solid-phase synthesis of π-conjugated oligomers to combinatorial library construction and screening. Chem Commun 2002;(10): 1015–23.
[17] Zhu J, Bienaymé H. Multicomponent reactions. Weinheim, Germany: Wiley-VCH Verlag GmbH & Co. KGaaA; 2005.
[18] Sunderhaus JD, Martin SF. Applications of multicomponent reactions to the synthesis of diverse heterocyclic scaffolds. Chem Eur J 2009;15(6):1300–8.
[19] Isambert N, Lavilla R. Heterocycles as key substrates in multicomponent reactions: the fast lane towards molecular complexity. Chem Eur J 2008;14(28):8444–54.
[20] Dömling A. Recent developments in isocyanide based multicomponent reactions in applied chemistry. Chem Rev 2006;106(1):17–89.
[21] Orru RVA, de Greef M. Recent advances in solution-phase multicomponent methodology for the synthesis of heterocyclic compounds. Synthesis 2003;2003 (10):1471–99.
[22] Bienaymé H, Hulme C, Oddon G, Schmitt P. Maximizing synthetic efficiency: multi-component transformations lead the way. Chem Eur J 2000;6(18):3321–9.
[23] Dömling A, Ugi I. Multicomponent reactions with isocyanides. Angew Chem Int Ed 2000;39(18):3168–210.
[24] Ugi I, Domling A, Werner B. Since 1995 the new chemistry of multicomponent reactions and their libraries, including their heterocyclic chemistry. J Heterocycl Chem 2000;37(3):647–58.
[25] Weber L, Illgen K, Almstetter M. Discovery of new multi component reactions with combinatorial methods. Synlett 1999;1999(03):366–74.
[26] Armstrong RW, Combs AP, Tempest PA, Brown SD, Keating TA. Multiple-Component condensation strategies for combinatorial library synthesis. Acc Chem Res 1996;29(3):123–31.
[27] Ugi I, Dömling A, Hörl W. Multicomponent reactions in organic chemistry. Endeavour 1994;18(3):115–22.
[28] Posner GH. Multicomponent one-pot annulations forming 3 to 6 bonds. Chem Rev 1986;86(5):831–44.
[29] D'Souza DM, Müller TJJ. Multi-component syntheses of heterocycles by transition-metal catalysis. Chem Soc Rev 2007;36(7):1095–108.
[30] Balme G, Bossharth E, Monteiro N. Pd-assisted multicomponent synthesis of heterocycles. Eur J Org Chem 2003;2003(21):4101–11.
[31] Battistuzzi G, Cacchi S, Fabrizi G. The aminopalladation/reductive elimination domino reaction in the construction of functionalized indole rings. Eur J Org Chem 2002;2002(16):2671–81.
[32] Niedballa J, Müller TJJ. Heterocycles by consecutive multicomponent syntheses via catalytically generated alkynoyl intermediates. Catalysts 2022;12(2):90.
[33] Biesen L, Müller TJJ. Multicomponent and one-pot syntheses of quinoxalines. Adv Synth Catal 2021;363(4):980–1006.
[34] Hassan S, Müller TJJ. Multicomponent syntheses based upon copper-catalyzed alkyne-azide cycloaddition. Adv Synth Catal 2015;357(4):617–66.

[35] Müller TJJ. Synthesis of carbo- and heterocycles via coupling-isomerization reactions. Synthesis 2012;44(02):159–74.
[36] Müller TJJ. Palladium-copper catalyzed alkyne activation as an entry to multicomponent syntheses of heterocycles. In: Orru RVA, Ruijter E, editors. Target in heterocyclic systems. Synthesis of heterocycles via multicomponent reactions II Berlin. Heidelberg: Springer Berlin Heidelberg; 2010. p. 25–94.
[37] Willy B, Müller TJJ. Multi-component heterocycle syntheses via catalytic generation of alkynones. Curr Org Chem 2009;13(18):1777–90.
[38] Müller TJJ. Multi-component synthesis of fluorophores via catalytic generation of alkynoyl intermediates. Drug Discov Today Technol 2018;29:19–26.
[39] Merkt FK, Müller TJJ. Solid state and aggregation induced emissive chromophores by multi-component syntheses. Isr J Chem 2018;58(8):889–900.
[40] Riva R, Moni L, Müller TJJ. Multicomponent strategies for the diversity-oriented synthesis of blue emissive heterocyclic chromophores. Targets Heterocycl Syst. 2016;20:85–112.
[41] Levi L, Müller TJJ. Multicomponent syntheses of fluorophores initiated by metal catalysis. Eur J Org Chem 2016;2016(17):2902–18.
[42] Tietze LF, Brasche G, Gericke KM, editors. Domino reactions in organic synthesis. Weinheim, Germany: Wiley-VCH Verlag GmbH & Co. KGaaA; 2006.
[43] Xu P-F, Wang W, editors. Catalytic cascade reactions. Hoboken, NJ, USA: John Wiley & Sons; 2014.
[44] Vlaar T, Ruijter E, Orru RVA. Recent advances in palladium-catalyzed cascade cyclizations. Adv Synth Catal 2011;353(6):809–41.
[45] Tietze LF. Domino reactions in organic synthesis. Chem Rev 1996;96(1):115–36.
[46] Tietze LF, Beifuss U. Sequential transformations in organic chemistry: a synthetic strategy with a future. Angew Chem Int Ed 1993;32(2):131–63.
[47] Tietze LF. Domino-reactions: the tandem-Knoevenagel-hetero-Diels-Alder reaction and its application in natural product synthesis. J Heterocycl Chem 1990;27(1):47–69.
[48] Schönhaber J, Müller TJJ. Luminescent bichromophoric spiroindolones – synthesis and electronic properties. Org Biomol Chem 2011;9(18):6196–9.
[49] D'Souza DM, Kiel A, Herten D-P, Rominger F, Müller TJJ. Synthesis, structure and emission properties of spirocyclic benzofuranones and dihydroindolones: a domino insertion–coupling–isomerization– Diels–Alder approach to rigid fluorophores. Chem Eur J 2008;14(2):529–47.
[50] Wilcke T, Postole A, Krüsmann M, Karg M, Müller TJJ. Amphipolar, amphiphilic 2,4-diarylpyrano[2,3-*b*]indoles as turn-ON luminophores in acidic and basic media. Molecules 2022;27(7):2354.
[51] Wilcke T, Glißmann T, Lerch A, Karg M, Müller TJJ. Acidochromic turn-on 2,4-diarylpyrano[2,3-*b*]indole luminophores with solubilizing groups for a broad range of polarity. ChemistrySelect 2018;3(37):10345–51.
[52] Schönhaber J, Frank W, Müller TJJ. Insertion−coupling−cycloisomerization domino synthesis and cation-induced halochromic fluorescence of 2,4-Diarylpyrano[2,3-*b*]indoles. Org Lett 2010;12(18):4122–5.
[53] Schönhaber J, D'Souza DM, Glißmann T, Mayer B, Janiak C, Rominger F, Frank W, Müller TJJ. Domino insertion–coupling synthesis of solid-state luminescent propynylidene indolones. Chem Eur J 2018;24(55):14712–23.
[54] Moni L, Denißen M, Valentini G, Müller TJJ, Riva R. Diversity-oriented synthesis of intensively blue emissive 3-hydroxyisoquinolines by sequential Ugi four-component reaction-reductive Heck cyclization. Chem Eur J 2015;21(2):753–62.
[55] Moni L, Gers-Panther CF, Anselmo M, Müller TJJ, Riva R. Highly convergent synthesis of intensively blue emissive furo[2,3-*c*]isoquinolines by a palladium-catalyzed cyclization cascade of unsaturated Ugi products. Chem Eur J 2016;22(6):2020–31.
[56] Luo R, Wang Z, Luo D, Qin Y, Zhao C, Yang D, Lu T, Zhou Z, Huang Z. Design, synthesis, and biological evaluation of novel triazoloquinazolinone derivatives as SHP2 protein inhibitors. J Enzym Inhib Med Chem 2021;36(1):2170–82.
[57] Ding D, Zhao Y, Meng Q, Xie D, Nare B, Chen D, Bacchi CJ, Yarlett N, Zhang Y-K, Hernandez V, Xia Y, Freund Y, Abdulla M, Ang K-H, Ratnam J, McKerrow JH, Jacobs RT, Zhou H, Plattner JJ. Discovery of novel benzoxaborole-based potent antitrypanosomal agents. ACS Med Chem Lett 2010;1(4):165–9.
[58] Klapars A, Buchwald SL. Copper-catalyzed halogen exchange in aryl halides: an aromatic Finkelstein reaction. J Am Chem Soc 2002;124(50):14844–5.
[59] Zhou P-X, Luo J-Y, Zhao L-B, Ye Y-Y, Liang Y-M. Palladium-catalyzed insertion of N-tosylhydrazones for the synthesis of isoindolines. Chem Commun 2013;49(31):3254–6.
[60] Park K, Palani T, Pyo A, Lee S. Synthesis of aryl alkynyl carboxylic acids and aryl alkynes from propiolic acid and aryl halides by site selective coupling and decarboxylation. Tetrahedron Lett 2012;53(7):733–7.
[61] Murata M, Watanabe S, Masuda Y. Novel palladium(0)-catalyzed coupling reaction of dialkoxyborane with aryl halides: convenient synthetic route to arylboronates. J Org Chem 1997;62(19):6458–9.
[62] Merkul E, Schäfer E, Müller TJJ. Rapid synthesis of bis(hetero)aryls by one-pot Masuda borylation–Suzuki coupling sequence and its application to concise total syntheses of meridianins A and G. Org Biomol Chem 2011;9(9):3139–41.
[63] Ponpandian T, Muthusubramanian S. Copper catalysed domino decarboxylative cross coupling-cyclisation reactions: synthesis of 2-arylindoles. Tetrahedron Lett 2012;53(32):4248–52.
[64] Fery-Forgues S, Lavabre D. Are fluorescence quantum yields so tricky to measure? A demonstration using familiar stationery products. J Chem Educ 1999;76(9):1260–4.
[65] Boens N, Qin W, Basarić N, Hofkens J, Ameloot M, Pouget J, Lefèvre J-P, Valeur B, Gratton E, vandeVen M, Silva ND, Engelborghs Y, Willaert K, Sillen A, Rumbles G, Phillips D, Visser AJWG, van Hoek A, Lakowicz JR, Malak H, Gryczynski I, Szabo AG, Krajcarski DT, Tamai N, Miura A. Fluorescence lifetime standards for time and frequency domain fluorescence spectroscopy. Anal Chem 2007;79(5):2137–49.
[66] Jones II G, Jackson WR, Choi CY, Bergmark WR. Solvent effects on emission yield and lifetime for coumarin laser dyes. Requirements for a rotatory decay mechanism. J Phys Chem 1985;89(2):294–300.
[67] Barlin GB, Brown WV. Kinetics of reactions in heterocycles. Part V. Replacement of the methylsulphinyl and methylthio-groups in substituted six-membered nitrogen heterocycles by methoxide ion. J Chem Soc B 1968:1435–45.
[68] Sigel H, Martin RB. Coordinating properties of the amide bond. Stability and structure of metal ion complexes of peptides and related ligands. Chem Rev 1982;82(4):385–426.
[69] Gaussian 16, Revision A.03, Frisch MJ, Trucks GW, Schlegel HB, Scuseria GE, Robb MA, Cheeseman JR, Scalmani G, Barone V, Petersson GA, Nakatsuji H, Li X, Caricato M, Marenich AV, Bloino J, Janesko BG, Gomperts R, Mennucci B, Hratchian HP, Ortiz JV, Izmaylov AF, Sonnenberg JL, Williams-Young D, Ding F, Lipparini F, Egidi F, Goings J, Peng B, Petrone A, Henderson T, Ranasinghe D, Zakrzewski VG, Gao J, Rega N, Zheng G, Liang W, Hada M, Ehara M, Toyota K, Fukuda R, Hasegawa J, Ishida M, Nakajima T, Honda Y, Kitao O, Nakai H, Vreven T, Throssell K, Montgomery JA, Peralta JE, Ogliaro F, Bearpark MJ, Heyd JJ, Brothers EN, Kudin KN, Staroverov VN, Keith TA, Kobayashi R, Normand J, Raghavachari K, Rendell AP, Burant JC, Iyengar SS, Tomasi J, Cossi M, Millam JM, Klene M, Adamo C, Cammi R, Ochterski JW, Martin RL, Morokuma K, Farkas O, Foresman JB, Fox DJ. Gaussian, Inc., Wallingford CT, 2016.
[70] Lee C, Yang W, Parr RG. Development of the Colle-Salvetti correlation-energy formula into a functional of the electron density. Phys Rev B 1988;37(2):785–9.
[71] Becke AD. A new mixing of Hartree–Fock and local density-functional theories. J Chem Phys 1993;98(2):1372–7.
[72] Becke AD. Density-functional thermochemistry. III. The role of exact exchange. J Chem Phys 1993;98(7):5648–52.
[73] Kim K, Jordan KD. Comparison of density functional and MP2 calculations on the water monomer and dimer. J Phys Chem 1994;98(40):10089–94.
[74] Stephens PJ, Devlin FJ, Chabalowski CF, Frisch MJ. Ab initio calculation of vibrational absorption and circular dichroism spectra using density functional force fields. J Phys Chem 1994;98(45):11623–7.
[75] Krishnan R, Binkley JS, Seeger R, Pople JA. Self-consistent molecular orbital methods. XX. A basis set for correlated wave functions. J Chem Phys 1980;72(1):650–4.
[76] Scalmani G, Frisch MJ. Continuous surface charge polarizable continuum models of solvation. I. General formalism. J Chem Phys 2010;132(11):114110.
[77] Caricato M, Mennucci B, Tomasi J, Ingrosso F, Cammi R, Corni S, Scalmani G. Formation and relaxation of excited states in solution: a new time dependent polarizable continuum model based on time dependent density functional theory. J Chem Phys 2006;124(12):124520.